JOURNAL OF PROPULSION AND POWER
Vol. 17, No. 2, March–April 2001

Gear Fault Detection in Rocket Engine Turbomachinery

S. J. DiMaggio,* S. Rubin,† and B. H. Sako‡
The Aerospace Corporation, Los Angeles, California 90009-2957

A method for detecting anomalous gear behavior in rocket engine turbomachinery during acceptance hot firing is presented. The diagnostic procedure is based on a cepstrum analysis of steady-state gearbox accelerations. In this application, the cepstrum is defined as the inverse discrete Fourier transform of the log of the two-sided autospectral density. The vibration measurements used in the analysis are acquired during static hot fire tests from accelerometers mounted on the external surface of the turbopump gearbox. Following the ground tests, the cepstrum technique is used to provide insight into the differences between turbopumps that have functioned nominally and those with out-of-family signatures. The effectiveness of the method is demonstrated by comparing analysis results from an engine in good condition with a similar engine that suffered complete gear failure during its development test. This example is used to suggest that the cepstrum method cannot only help detect out-of-family vibration characteristics, but can also provide insight into the nature of a defect. A source mechanism is proposed to explain the unique spectral characteristics that appear due to the presence of the gear fault.

Nomenclature

A	=	amplitude of force input, lbs
$\hat{A}$	=	amplitude of force input, lbs^2/Hz
C_{yy}	=	output cepstrum
F	=	input force, lbs
$\hat{F}$	=	autospectral density (ASD) of input force, lbs^2/Hz
f_k	=	discrete frequencies, Hz
f_{LOX}	=	frequency of liquid oxygen (LOX) shaft rotation, Hz
f_n	=	natural frequency, Hz
H_d	=	system defect transfer function
H_i	=	system i transfer function
H_i^*	=	conjugate transpose of H_i
j	=	integers
N	=	number of data values per segment
n	=	output noise, g
n_d	=	number of segments per data record
S_{dd}	=	ASD of defect input, g^2/Hz
S_{ii}	=	ASD of input i g^2/Hz
S_{ik}	=	cross-spectral density of i and k, g^2/Hz
S_{nn}	=	ASD of noise, g^2/Hz
S_{yy}	=	ASD of output, g^2/Hz
S_{yy}^d	=	ASD of defect output, g^2/Hz
S_{yy}^h	=	ASD of nominal system output, g^2/Hz
T	=	length of single data record segment, s
X_m	=	Fourier components of mth record
x_i	=	multiple inputs, g
y	=	output, g
y_d	=	output due to defect, g
α	=	pseudoacceleration scale factor
Δt	=	sampling rate, s
δ	=	dirac delta function
ς	=	coefficient of critical damping
τ	=	periodic time, s
$\Im^{-1}$	=	inverse discrete Fourier transform operator

Received 4 October 1999; revision received 19 April 2000; accepted for publication 25 April 2000.

*Senior MTS, Environmental Test and Ordnance Department, P.O. Box 92957. Member AIAA.

†Consultant, Structural Mechanics Subdivision, P.O. Box 92957. Associate Fellow AIAA.

‡Senior Engineering Specialist, Structural Dynamics Department, P.O. Box 92957. Member AIAA.

Introduction

TO gain insight into the behavior of a rocket engine prior to flight, vibration response data are acquired during acceptance tests known as static firings or hot runs. During these runs, the engine is fixed in a test stand and ignited. The steady-state data acquired are then analyzed to determine quantitative parameters that are used to assess an engine's vibration signature. In many cases of rotating machinery analysis, particular vibration signatures are related to specific types of component defects. For example, discrete gear tooth defects are often characterized in the frequency domain by the appearance of spectral components at higher order harmonics of the speed of the shaft upon which the faulty gear is located. It appears that the cepstrum analysis method, in addition to being helpful in detecting anomalous vibration signatures, also provides a diagnostic capability that gives information as to the nature of a defect so that proper corrective actions can be implemented. The use of the cepstrum method to detect and operate on a periodic family in the frequency domain has evolved[1,2] since its first introduction as the autospectrum of the logarithmic autospectrum.[3] In this paper, the cepstrum is implemented as the inverse discrete Fourier transform (IDFT) of the log of the two-sided autospectral density (ASD). Regardless of the form of the cepstrum used, the benefit of the method is its ability to detect and quantify periodic families in the frequency domain.

Vibration measurements are commonly used in many industries to evaluate the condition of rotating equipment.[4–7] There are many references[8–11] that discuss the relative merits of different techniques for detection and diagnosis of various types of machinery defects. A comprehensive listing of all of these references is, however, beyond the scope of this paper. This review of the relevant literature will focus on the cepstrum method and on detection of gear faults similar to the example that will be presented herein. The simplest fault detection techniques use the change in statistical properties of the vibration signal itself as a measure of engine health. Relevant vibration parameters that have been used include both the root mean square value[12] and the kurtosis.[10] While these parameters provide a single number that can potentially indicate a defect in the system, they cannot identify the source leading to a change in vibration level. Some gear fault detection methods[13] use the analytic (envelope) signal to provide information on the modulation of the gear mesh frequency (GMF). Because the operating speeds of rocket engine turbopumps are extremely high, measurement of the vibration environment up to the GMF is often beyond the capability of the data acquisition instrumentation, as will be the case in the example presented in this paper. More recently, the use of wavelet transforms has been proposed for gear fault detection.[14] References 9 and 10 provide a good overview of a variety of methods

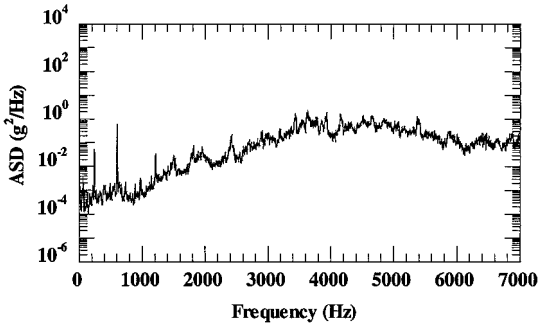

Fig. 1 ASD for static firing of a turbopump during nominal operating conditions.

used specifically to identify gear defects. A comprehensive review of the methods used in general machinery analysis and monitoring is given in Ref. 15.

Ground Test Data

The purpose of this paper is to propose a method that uses vibration measurements acquired during static firing tests to develop screening parameters that are related to the condition of turbomachinery components. These parameters are developed by operating on an acceleration measured during steady-state test conditions. The main difficulty is that these measurements are acquired on the exterior of the gearbox and, thus, vibrations induced by small defects in the internal components are often hidden within the high amplitude signal that is inherent in nominally operating rocket engines.

A representative ASD plot corresponding to a 4-s time frame and data acquired at a rate of 25,575 samples per second is shown in Fig. 1. These data were acquired during the final static firing of a production engine that operated nominally during its acceptance tests and later performed successfully during flight. The ASD is calculated via the finite Fourier transform method using 8192 data points and a Hanning window to suppress sidelobe leakage. Several distinct peaks can be seen in the low frequency regime that are a result of known forced system responses due to shaft rotation. Depending on the construction of the turbopump, other forced responses due to rotating components or flow-induced vibrations are often observed. In the case of this engine, the ASDs did not change significantly over the series of hot runs performed.

The results from the aforementioned engine will be compared to results obtained from a similar development engine that exhibited a failure of its liquid oxygen (LOX) gear at the end of a series of twenty-seven static firings. In the following sections, the final three static firings, denoted SF25, SF26, and SF27, will be used to demonstrate the method proposed in this paper. Subsequent to the failure during SF27, analysis and laboratory testing attributed the failure to a fatigue crack that progressed from the root of a single tooth on the LOX gear. Thus, the theoretical development will focus on developing a source mechanism that correlates the vibration induced by a discrete gear tooth fault to the unique spectral characteristics that appear in SF25–SF27.

Theoretical Development

This section focuses on the development of a simple input-output model that will be used to suggest a source mechanism for the spectral characteristics observed on an engine with a gear tooth fault. Following directly from Ref. 16, consider a data record $x(t)$ that is divided into n_d contiguous segments of length T. Each record segment $x_m(t)$ can be represented in digital terms, with a sampling interval of Δt, by N data values $\{x_{mn}\}$, where $n = 0, \ldots, N-1$ and $m = 1, \ldots, n_d$. The two-sided ASD is then defined

$$S_{xx}(f_k) = \frac{1}{n_d T}\sum_{m=1}^{n_d} |X_m(f_k)|^2, \qquad k = -\frac{N}{2}+1, \ldots, \frac{N}{2} \tag{1}$$

where X_m are the discrete Fourier components of the mth record. In all cases where the ASD is presented graphically, the one-sided ASD will be used.

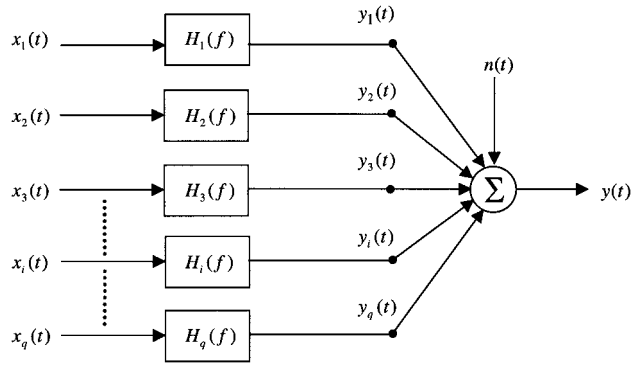

Fig. 2 Multi-input single-output (MISO) system.

As suggested in the abstract, measurements obtained from a particular accelerometer, or output, mounted on the exterior of a rocket engine turbopump are used to aid in the development of screening criteria for an engine. This output is a function of the various vibration-producing mechanisms, or inputs, within the gearbox. Therefore, this system can be described using the multi-input single-output (MISO) model shown in Fig. 2. For a more detailed derivation of the MISO model that follows, the reader is again referred to Ref. 16. Consider q transfer functions for the constant parameter linear systems $H_i(f)$, $i = 1, \ldots, q$, with q inputs $x_i(t)$, $i = 1, \ldots, q$, and one output $y(t)$. The output noise term $n(t)$ accounts for all deviations from the ideal model, which may be due to unmeasured inputs, nonlinear operations, non-stationary effects, and instrument noise. Assuming that $n(t)$ is uncorrelated with each $x_i(t)$, the basic frequency domain relation between the output ASD and the $i = 1, \ldots, q$ input ASDs is

$$S_{yy}(f) = \sum_{i=1}^{q}\sum_{k=1}^{q} H_i^*(f)H_k(f)S_{ik}(f) + S_{nn}(f) \tag{2}$$

where $S_{ik}(f)$ is the cross-spectral density function of $x_i(t)$ and $x_k(t)$, H^* is the conjugate transpose of H, and $S_{nn}(f)$ is the autospectral density of the noise.

Now consider a system whose output ASD is the summation of contributions from inputs $x_i(t)$, $i = 2, \ldots, q$, due to nominal system operation and a single input $x_1(t) = x_d(t)$ that is the result of some defect in the system. This system is approximated by assuming that the input arising from the defect is uncorrelated with the inputs due to nominal system performance. In mathematical terms, this approximation means

$$S_{di}(f) = S_{id}(f) = 0, \qquad i = 2, \ldots, q \tag{3}$$

Substituting Eq. (3) into Eq. (2) yields

$$S_{yy}(f) = \sum_{i=2}^{q}\sum_{k=2}^{q} H_i^*(f)H_k(f)S_{ik}(f) + S_{nn}(f) + |H_d(f)|^2 S_{dd}(f) \tag{4}$$

where $S_{dd}(f)$ is the input ASD resulting from a defect in the system. Equation (4) can be rewritten

$$S_{yy}(f) = S_{yy}^h(f) + S_{yy}^d(f) \tag{5}$$

where the part of the total output ASD resulting from noise and nominal system operation is

$$S_{yy}^h(f) = \sum_{i=2}^{q}\sum_{k=2}^{q} H_i^*(f)H_k(f)S_{ik}(f) + S_{nn}(f) \tag{6}$$

and the contribution from the defect is

$$S_{yy}^d(f) = |H_d(f)|^2 S_{dd}(f) \tag{7}$$

Equations (5–7) show that the output ASD is a summation of contributions from nominal system operation, noise and the contribution from the defect in the system. Note that $S_{dd}(f)$, or the ASD of the

defect input, is amplified or attenuated by the magnitude of its associated transfer function $|H_d(f)|^2$. This relationship is important because it shows how a relatively low-level input phenomenon arising from a minor defect can be detected in the vicinity of a system resonance. A succinct discussion on how this amplification effect can be used to detect defects in turbopump bearings is given in Ref. 17 and is reviewed here as it applies to gear fault detection.

In the case of a defect in a gear tooth, a fundamental problem in detecting the anomaly using vibration measurements acquired on the pump housing is that the change in vibration level due to the small defect is often masked by nominal turbopump response at the fundamental defect frequency. If the force induced by a defect in a gear tooth is characterized by a short-duration impulse, however, the resulting energy will be spread across a wide region of the output spectrum. This situation is similar to that which is encountered in structural modal testing in which the structure is excited by a short duration force impulse that is meant to excite system resonances across a wide frequency band. The resonances that are excited depend on the impulse location and the amount of energy imparted to the system. Similarly, the impulse induced by the gear tooth defect can excite certain system resonances, and thus be amplified, across a wide frequency range. In this sense, the structural system itself acts as a mechanical amplifier for detecting the presence of the defect. Furthermore, because the response to the impulse is spread across a wide spectrum, detection techniques can be focused in frequency regimes where the defect is not masked by nominal vibratory response of the pump. The use of system resonances to amplify defects is also discussed in Ref. 18 as it applies to bearing fault detection. Based on the model proposed in Fig. 2, an additional consequence of the system resonance amplification is that the signal-to-noise ratio for the output due to the defect is increased in the vicinity of the resonance.

One goal of a turbopump vibration diagnostic routine is to determine the nature of a defect by monitoring the change in output characteristics of the accelerometer. In this case, that means being able to relate a change in $S_{yy}(f)$ to a known defect condition. In the MISO model proposed, the input and output contributions $i = 2, \ldots, q$ are associated with nominal system operation. It is therefore reasonable to expect that, for consistent operating conditions, any major deviation in the total output, or $S_{yy}(f)$, will be a result of the single-input, single-output (SISO) defect system ($i = 1 = d$) described in the frequency domain by Eq. (7). Therefore, concentration is placed on postulating a defect SISO that can be shown to correlate with a change in the output vibration spectrum for SF25–SF27.

To understand the transmission path effects between the defect location, or LOX gear, and the accelerometer, system identification methods such as tap tests and analytical analyses including the gearbox could help in estimating the transfer function $H_d(f)$ associated with the defect SISO. In the case of the following example, these results were not originally available due to constraints beyond the analyst's control. Therefore, a simple single degree-of-freedom (SDOF) model is proposed to characterize the defect SISO. It should be understood that this model is not intended to be a physical representation of the turbopump but, rather, is a means by which the transfer function associated with the defect can be mathematically described. This SDOF model is governed by the following equation:

$$\ddot{y}_d + 2\varsigma(2\pi f_n)\dot{y}_d + (2\pi f_n)^2 y_d = (1/m)F \tag{8}$$

where F is the force input induced by the defect and $\ddot{y}_d$ is the defect contribution to the total response acceleration. The transfer function relating the input and output is characterized by the natural frequency f_n, the coefficient of critical damping ς, and the system mass m. An estimate of the natural frequency that best describes the physical system is made by performing a waterfall analysis of the SF25 shutdown time transient shown in Fig. 3. The SF25 transient is presented in a max-mean-min format that essentially provides the envelope and mean of the time history within 20 ms time intervals. The contour waterfall plot of spectral density for this transient is shown in Fig. 4, in which the lightest regions represent the highest spectral density. Between 182 and 183 s the

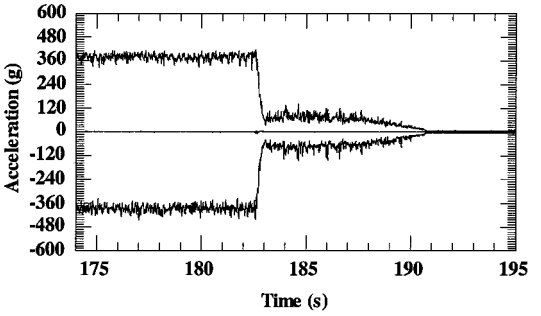

Fig. 3 Shutdown transient for SF25.

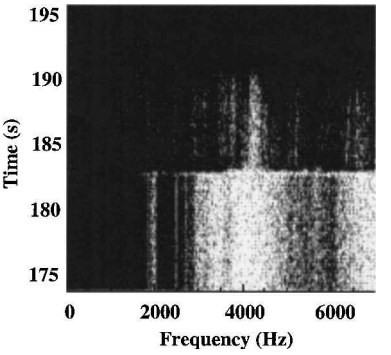

Fig. 4 Contour waterfall plot of SF25 shutdown transient.

engine is shut down and the high-amplitude forced responses due to shaft rotations and flow-induced vibration are no longer evident. Following the shutdown, however, significant vibration at system resonances can still be observed in the regions of 4200 Hz and, to a lesser extent, at other frequencies. Because the relatively wideband peak at 4200 Hz appears consistently in the shutdown waterfall plots, regardless of engine operating condition, it is believed that the 4200 Hz resonance is probably a gearbox housing structural resonance. This belief is reinforced by the observation that the measured output ASDs at all observed operating conditions are characterized by a shape containing a wideband maximum at 4200 Hz (see Fig. 1). Therefore, this structural resonance is believed to be in the transmission path between all mechanical and flow-induced inputs and the output. This belief has been further reinforced by results obtained from a tap test of limited scope in which 22 locations on the turbopump exterior were impacted with an instrumented force hammer. Regardless of impact location, the frequency response function magnitude relating the acceleration response on the gearbox to the short duration force impulse was consistently characterized by a peak at 4200 Hz that dominated the spectrum. Thus, due to lack of additional system identification information that could be used to uniquely define the defect SISO, a value of 4200 Hz is used for the natural frequency of the SDOF defect model. Note that the frequencies observed in the waterfall contours are actually the damped natural frequencies of the system. For this application and at critical damping values of less than 10%, the difference between damped and undamped natural frequencies is negligible. A value of $\varsigma = 0.04$ is used for this system based on curve-fitting the results of this theory with ground test results to be presented in a later section. Values for ς from 0.01 to 0.10 were investigated, with the value of 0.04 seeming to best fit the actual data. At this point, the SDOF transfer function magnitude squared, or $|H_d(f)|^2$, is defined for a unit mass of 1 pound as shown in Fig. 5.

Now consider a LOX gear containing a tooth defect that induces a short-duration force impulse once per revolution of the LOX shaft. Mathematically this means that the forcing function is defined

$$F(t) = A\delta(t - j/f_{\mathrm{LOX}}) \tag{9}$$

where A is the amplitude of the force impulses, δ is the dirac delta function, j is any integer, and f_{LOX} is the frequency of rotation of the LOX shaft. This input forcing function is characterized by

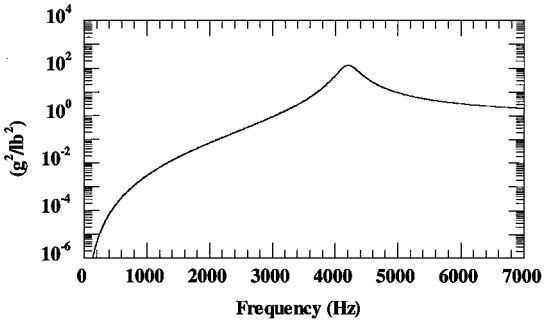

Fig. 5 Transfer function magnitude squared for SDOF defect model with unit mass.

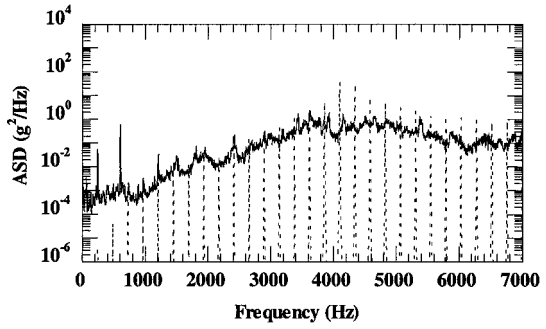

Fig. 6 ASD of SDOF response to series of impulses for $\alpha = 100$ plotted on the same scale as the healthy turbopump ASD of Fig. 1.

constant amplitude impulses spaced at the reciprocal of the LOX shaft rotation rate. The corresponding ASD of this defect input is characterized by energy spread across the entire frequency spectrum and contained in constant amplitude spikes located at the fundamental and integer multiples of the LOX shaft rotation rate. Mathematically, this ASD can be defined

$$\hat{F}(f) = \hat{A}\delta(f - jf_{\mathrm{LOX}}) \tag{10}$$

where $\hat{A}$ is the amplitude of the spikes in the ASD. The response of the SDOF oscillator to the input in Eq. (9) is governed by the following equation:

$$\ddot{y}_d + 2\varsigma(2\pi f_n)\dot{y}_d + (2\pi f_n)^2 y_d = \alpha\delta(t - j/f_{\mathrm{LOX}}) \tag{11}$$

where $\alpha = A/m$ is a scale factor that can be thought of as a pseudoacceleration that depends on the amplitude of the force impulses and the unknown system constant associated with the reciprocal of the SDOF's mass. The time domain response of the SDOF oscillator, described mathematically by Eq. (11), is characterized by an exponentially decaying oscillatory response at the 4200 Hz natural frequency that repeats at the impact spacing of $1/f_{\mathrm{LOX}}$. Using Eq. (7), notice in the frequency domain that the output ASD due to the defect, or $S^d_{yy}(f)$, is the product of the input defect ASD and its associated transfer function magnitude squared (shown in Fig. 5). This output ASD due to a theorized LOX gear defect at a shaft rotation rate of $f_{\mathrm{LOX}} = 241$ Hz and a pseudoaccelerationlevel of $\alpha = 100$ gs is shown in Fig. 6 with a dotted line. To facilitate discussions later in the paper, the ASD of the nominally operating turbopump (shown in Fig. 1) is also presented in the figure with a solid line. While it may initially be counterintuitive, Fig. 6 indicates that the contribution to the output spectrum due to the defect is smallest at the fundamental defect frequency and largest at significantly higher frequencies near the system resonance. Figure 6 also shows that the change in $S_{yy}(f)$ due to a defect in a LOX gear tooth can be characterized by an increase in the spectrum at fundamental and integer multiples of the LOX shaft rotation rate. Furthermore, the increase at these LOX harmonics will not be uniform across the spectrum but, rather, will be amplified and/or attenuated by the transfer function associated with the defect.

The consequence of this non-uniform increase is that the defect signal-to-noise ratio will be largest in the regions surrounding the system resonance and smallest at the fundamental frequency of the defect. It is therefore reasonable to expect that, if a gear fault were to exist in an actual turbopump, the harmonics of the defect frequency would be most evident near the system resonance. This relationship is also indicated in Fig. 6 by observing that the peaks due to the theorized defect are larger than the ASD levels corresponding to nominal system response only in the region of the structural resonance. It will be shown that this region is the one in which the LOX gear harmonics first appear in the actual engine containing the gear fault.

In order for a particular mechanical or flow-induced input to be amplified by the 4200 Hz resonance, it must have an input spectrum containing energy at that frequency. On the one hand, inputs associated with nominal operation of the turbopump consistently contain energy in the lower frequency regime whereas the energy content in the higher frequency regime (ie. near the 4200 Hz resonance) is typically not as large. On the other hand, the short duration, albeit low amplitude, inputs that characterize the disturbance induced by a discrete gear tooth defect are characterized by a spectrum with potentially significant energy content at higher frequencies. In fact, as one approaches the theoretical dirac delta input that is proposed in Eq. (9), the energy content is equally distributed across the entire frequency range and is contained in spikes at the fundamental and integer multiples of the defect frequency. By virtue of this argument, it can be suggested that identification of defects near 4200 Hz may be more effective because the defects are not hidden or masked by the inputs due to a nominally operating engine (as they might in the lower frequency range). Therefore, it is suggested that gearbox acceleration outputs be processed over a frequency range that includes system resonant frequencies that may be helpful in identifying faults. As a case in point, prior to the failure described in this paper, data analysis was carried out only to 2000 Hz, a procedure that reduced the ability to detect impending failure, as will be seen in the next section.

Gear Failure Example

As previously mentioned, actual ground test data from static firings SF25–SF27 are used to assess the defect model postulated in the previous section. Recall that this engine was characterized by a complete failure of its LOX gear at the end of SF27. It is postulated that, as engine operating time increased from SF25 to SF27, a local LOX gear tooth defect grew until the gear failed. It is also suggested that, as the defect evolved, the force induced by the defect consequently increased. In relation to the theoretical development in the previous section, these relationships imply that, as the defect becomes more severe, the amplitude A of the force impulses defined in Eq. (9) and thus, the scale factor α in (11), become larger. The solid lines in Figs. 7–9 are the output ASDs taken during consistent operating conditions for SF25–SF27 respectively. Additionally, the dotted lines in Figs. 7–9 show the ASDs corresponding to the theoretical contribution of the defect for values of $\alpha = 70$, 100, and 200 gs respectively. In these three figures, the rotation rate, and thus the defect impulse rate, of the LOX shaft is approximately 241 Hz. Recall from Eqs. (4–7) that the theoretical portion of the figures is

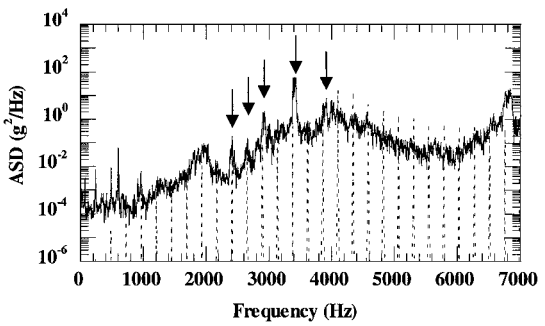

Fig. 7 Comparison of SF25 ASD with theoretical prediction of defect contribution corresponding to $\alpha = 70$.

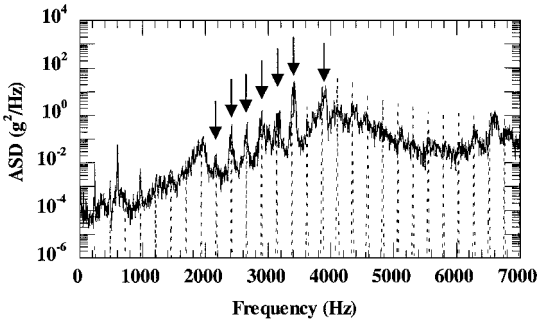

Fig. 8 Comparison of SF26 ASD with theoretical prediction of defect contribution corresponding to $\alpha = 100$.

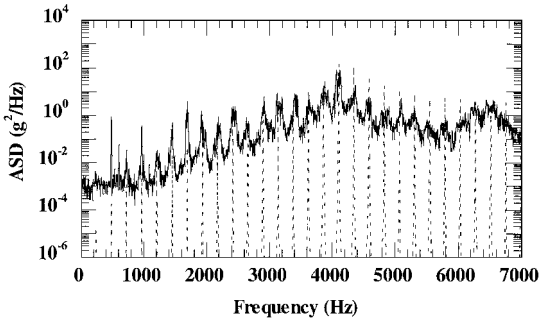

Fig. 9 Comparison of SF27 ASD with theoretical prediction of defect contribution corresponding to $\alpha = 200$.

the defect's contribution to the total ASD. This portion of the response must be added to the ASD of the nominally operating system to get the total ASD of the output. Also, recall that an ASD for a nominally operating engine is shown in Fig. 1. Note the increase in amplitude of the spectral components corresponding to integer multiples of the defect frequency as engine operating life increases from SF25 through SF27. These spectral components are indicated with arrows in Figs. 7 and 8. Further, note that the initial and most pronounced changes occur not at the fundamental defect frequency (241 Hz), but, rather, above 2000 Hz, as the frequencies increase toward the system resonance identified using the waterfall contour plot of Fig. 4. In fact, the spectral lines corresponding to the fundamental frequency of LOX shaft rotation and its lowest harmonics do not appear to increase at all until SF27. This is consistent with the theoretical development.

Based on the results presented in Figs. 7–9, it appears that the postulated model provides helpful insight into the physics of the process. There are two possible reasons why the hypothesized model, involving an ideal delta function force and a single transmission resonance of 4200 Hz, leads to an overestimation of defect-based harmonics above the 4200 Hz range relative to those in the 2000–4200 Hz range (see Figs. 7–9). One reason is that the use of an SDOF model may lead to an overemphasis of the frequency response function associated with the defect in the region near 4200 Hz. The other possibility is that the defect forcing function has a very short, yet finite, pulse duration, rather than the assumed ideal delta function. This may, in turn, lead to a frequency spectrum characterized by spectral components with diminished amplitudes at frequencies above 4200 Hz. Nevertheless, the model presented does lead to results that provide reasonably good correlation with the actual data.

Cepstrum Method

Although the change in visual characteristics of the ASD is helpful in providing a qualitative indication of a potential defect, it is desirable to quantify the degree of abnormality of the vibration signature. It is further useful if this abnormality can be quantified using a single parameter that can be stored in a database and used to make comparisons between those engines that have operated nominally and those engines that have exhibited known defects. The cepstrum method is presented as a technique that provides a single quantitative parameter that appears to be related to the presence and growth of a discrete gear tooth defect.

In many cases of machinery analysis, fault development appears in the frequency spectrum as a family of harmonics or sidebands that are spaced at multiples of the fundamental frequency of the disturbance induced by the defect. This relationship was demonstrated in the previous section for the particular case of a LOX gear tooth defect. The cepstrum method has been used to detect and quantify these harmonics in cases of damage to both rolling-element bearings[19] and gears.[20–22] As a gear fault evolves, the harmonic pattern in the ASD can often be identified visually, as shown in the previous section. By performing a cepstrum analysis, however, the strength of an entire family of harmonics is expressed in one component in the cepstral domain. Using the cepstrum can aid the analyst in quantifying the severity of the defect and monitoring the defect evolution using the magnitude of a single cepstrum component. Two additional advantages of using the cepstrum are that the frequency spacing of a periodic family can be precisely determined, and the appearance of harmonics can often be detected earlier than by using visual inspection of the ASD.

The form of the cepstrum used by different researchers tends to vary depending upon the specific application. After investigation of several cepstrum implementations, the form of the two-sided cepstrum, consistent with the notation in Eq. (1), that is used in this paper is defined by

$$C_{yy}(\tau_n) = \Im^{-1}\{\log[S_{yy}(f_k)]\} = \Delta f \sum_{k=-N/2+1}^{N/2} \{\log[S_{yy}(f_k)]\} e^{j2\pi kn/N}$$

$$n = -N/2 + 1, \ldots, N/2 \quad (12)$$

at the discrete periodic times $\tau_n = n/N\Delta f$ where Δf is the line spacing of the ASD and $\Im^{-1}$ denotes the inverse discrete Fourier transform operator. Note that the cepstrum differs from the autocorrelation function only by virtue of the logarithmic conversion of the ASD before the IDFT is performed. Since the cepstrum is the IDFT of a function of frequency, its independent variable τ_n is actually time. The parameter τ_n, however, can better be thought of as a delay time, as for the autocorrelation function. Therefore, although most researchers refer to τ_n as "quefrency," it seems more appropriate to use the term "periodic time," as suggested in Ref. 2. Note that, if the log of the ASD is periodic in nature with a frequency spacing of f_P, the contribution of all of the harmonics will be concentrated in the single cepstrum component $C_{yy}(\tau_P)$ at a value of $\tau_P = 1/f_P$. The cepstrum defined in Eq. (12) is a real-valued, two-sided, even function that is computed using the two-sided ASD defined in Eq. (1). Whenever the output cepstrum is presented graphically, however, the magnitude of only one side will be shown.

Most analysts use the one-sided ASD and the one-sided cepstrum for computation purposes. By using the two-sided ASD in the cepstrum definition in Eq. (12), however, the resolution of the cepstrum is increased by a factor of two, while the characteristics of the ASD itself remain relatively unchanged. This resolution is important in the current application of the cepstrum due to the high operating speeds of the turbopump and the wide range of component defect frequencies that are of interest. In what follows, the magnitude of the two-sided cepstrum components, or $|C_{xx}(\tau_n)|$, will be used to identify and track the LOX gear fault of the previous section. To establish a baseline, the cepstrum corresponding to the nominally operating turbopump ASD shown in Fig. 1 is presented in Fig. 10. The absence of an identifiable peak at the LOX periodic time in the figure should be noted.

The cepstrum plots corresponding to the ASDs shown in Figs. 7–9 are presented in Figs. 11–13 respectively. Notice the increase in the cepstral component corresponding to a periodic time of $1/f_{\mathrm{LOX}} \cong 0.00415 \times 10^{-3}$ s. These plots indicate that this component is related to the growth in the frequency domain of the spectral components at fundamental and integer multiples of the defect frequency. Furthermore, by virtue of the previous correlation between

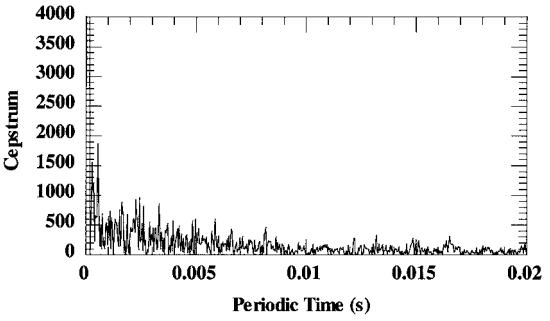

Fig. 10 Cepstrum for nominally operating turbopump. Note the absence of a significant cepstrum component corresponding to the reciprocal of the LOX shaft frequency (1/241 or 0.00415).

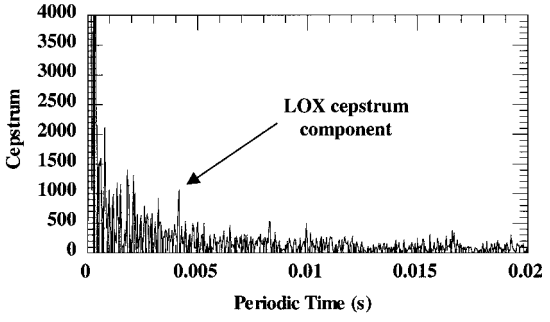

Fig. 11 Cepstrum for SF25. Note the emergence of the defect-induced component.

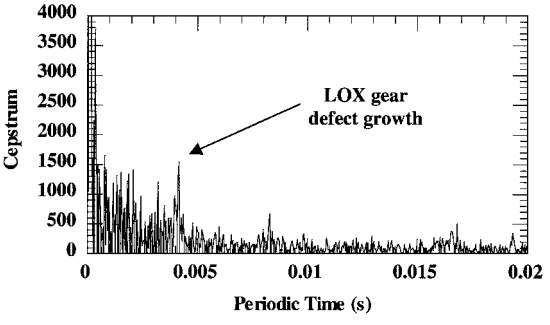

Fig. 12 Cepstrum for SF26. Note the growth of the defect-induced component.

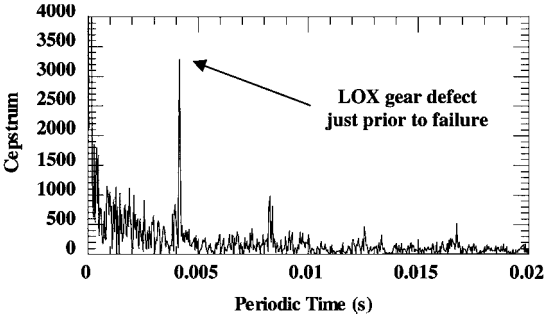

Fig. 13 Cepstrum for SF27. Note the continued growth of the cepstrum component corresponding to the reciprocal of the defect frequency.

the growth of these harmonics in the spectral domain and a defect in the LOX gear tooth, this single parameter, therefore, appears to be related directly to the evolution of a LOX gear fault.

A major benefit of the cepstrum method is its ability to provide insight into the nature of a defect, as opposed to indicating only that a problem exists. More specifically, the periodic time at which the cepstrum component grows is directly related to the frequency of the particular shaft containing the defect. If there were a defect in a gear tooth on a shaft other than the LOX pump's, it would be reasonable to expect a similar growth of the cepstrum component associated with the inverse of that shaft's rotation rate. In this sense, the cepstrum method is not only a detection technique, but also a diagnostic tool.

Conclusions

The cepstrum method has been shown to be capable of detecting anomalous gear behavior in a particular rocket engine turbopump. The method has been used to generate a parameter that can be stored in a database and that appears to be directly related to a gear defect. A source mechanism has been proposed to explain the appearance of higher order harmonics inherent in an ASD for a turbopump with a faulty gear. This source mechanism provides a reasonable expectation that similar defects in other turbopump gears may also be detected. This identification would be accomplished by tracking the cepstrum component corresponding to the inverse of the rotation rate of the shaft supporting the gear in question. The theoretical development also provides a rationale for suggesting that certain types of component defects may be more easily detected in frequency regimes corresponding to known system resonances than at the fundamental defect frequency. Additionally, an understanding of the source mechanism appears to provide information about the most effective placement of instrumentation when designing a rocket engine acceptance screening program. Based on the previous discussion, it seems advantageous to place several accelerometers in locations on the exterior of the gearbox housing that are characterized by significant system resonances.

Acknowledgments

This work was supported by the U.S. Air Force Material Command, Space and Missile Systems Center, under Contract F04701-93-C-0094. The authors would like to thank Z. H. Duron for many helpful discussions.

References

[1]Oppenheim, A. V., and Schafer, R. W., "Cepstrum Analysis and Homomorphic Deconvolution," *Discrete-Time Signal Processing*, Prentice–Hall, Englewood Cliffs, NJ, 1989, Chap. 12.

[2]Randall, R. B., *Frequency Analysis*, 3rd edition, Bruel and Kjaer, Naerum, Denmark, Sept. 1987.

[3]Bogert, B. P., Healy, M. J. R., and Tukey, J. W., "The Quefrency Analysis of Time Series for Echoes: Cepstrum, Pseudo-Autocovariance, Cross-Cepstrum and Saphe Cracking," *Proceedings of Symposium on Time Series Analysis*, Wiley, New York, 1963, pp. 209–243.

[4]Bradshaw, P., and Randall, R. B., "Early Detection and Diagnosis of Machine Faults on the Trans Alaska Pipeline," MSA Session, ASME Conf., Dearborn, MI, 11–14 Sept. 1983.

[5]Bate, A. H., "Vibration Diagnostics for Industrial Electric Motor Drives," *Bruel and Kjaer Application Note*, Naerum, Denmark.

[6]Kryter, R. C., and Haynes, H. D., "Condition Monitoring of Machinery Using Motor Current Signature Analysis," *Sound and Vibration*, Vol. 23, No. 9, 1989, pp. 14–26.

[7]Lyon, R. H., "Damage Detection and Identification in Structures and Mechanisms," *Proceedings of the 15th International Modal Analysis Conference*, Vol. 1, Society for Experimental Mechanics, Orlando, FL, 1997, pp. 28–32.

[8]Courrech, J., "Condition Monitoring of Machinery," *Shock and Vibration Handbook*, 4th edition, McGraw–Hill, New York, 1996, Chap. 16.

[9]Zakrajsek, J. J., and Lewicki, D. G., "Detecting Gear-Tooth Fatigue Cracks in Advance of Complete Fracture," NASA TM 107145, NASA Tech Briefs, LEW-16433, 1996.

[10]Brennan, M. J., Chen, M. H., and Reynolds, A. G., "Use of Vibration Measurements to Detect Local Tooth Defects in Gears," *Sound and Vibration*, Vol. 31, No. 11, 1997, pp. 12–17.

[11]Leuridan, J., Van der Auweraer, H., and Vold, H., "The Analysis of Non-Stationary Dynamic Signals," LMS International Application Note, 1994, pp. 1–20.

[12]International Standard (ISO) 3945, "Mechanical Vibration of Large Rotating Machines with Speed Range from 10 to 200 Rev/s: Measurement and Evaluation of Vibration Severity in Situ," Ref. ISO 3945-1977(E), 1978.

[13]McFadden, P. D., "Detecting Fatigue Cracks in Gears by Amplitude and Phase Demodulation of the Meshing Vibration," *Journal of Vibration, Acoustics, Stress, and Reliability in Design*, Vol. 108, 1986, pp. 165–170.

[14]Staszewski, W. J., and Tomlinson, G. R., "Application of the Wavelet Transform to Fault Detection in a Spur Gear," *Mechanical Systems and Signal Processing*, Vol.'8, No. 3, 1994, pp. 289–307.

[15]Mitchell, J. S., *Machinery Analysis and Monitoring*, PennWell Publ. Co., Tulsa, OK, 1981, pp. 1–374.

[16]Bendat, J. S., and Piersol, A. G., *Random Data Analysis and Measurement Procedures*, 2nd edition, Wiley, New York, 1986, pp. 201–207.

[17]Tecza, J. A., Ensegi, M., Hanson, R., Hoogenboom, L., Martin, M., and Cowper, L., *Rocket Engine Turbopump Bearing Diagnostics*, Astronautics Lab. (AFSC) TR AL-TR-89-042, Aug. 1989, pp. 165, 166.

[18]Lyon, R. H., *Machinery Noise and Diagnostics*, Butterworths, London, 1987.

[19]Courrech, J., "New Techniques for Fault Diagnosis in Rolling Element Bearings," *Proceedings of the 40th Meeting of the Failure Preventive Group*, National Bureau of Standards, Gaithersburg, MD, 16–18 April 1985, pp. 83–91.

[20]Randall, R. B., "Cepstrum Analysis," *Bruel and Kjaer Technical Review*, No. 3, 1981, pp. 1–41.

[21]Randall, R. B., "Ceptrum Analysis and Gearbox Fault Diagnosis," *Bruel and Kjaer Application Note*, No. 233-80.

[22]Randall, R. B., "A New Method for Modeling Gear Faults," *Journal of Mechanical Design*, Vol. 104/259, April 1982, pp. 259–267.